www.czasopisma.pan.pl PAN POLSKA AKADEMIA NAUK www.journals.pan.pl

A R C H I V E S O F M E T A L L U R G Y A N D M A T E R I A L S

Volume 60 2015 Issue 1

DOI: 10.1515/amm-2015-0064

F. TREQUATTRINI*, A. PAOLONE**, O. PALUMBO**, F.M. VITUCCI**, M.A. NAVARRA***, S. PANERO***

LOW FREQUENCY MECHANICAL SPECTROSCOPY STUDY OF THREE PYRROLIDINIUM BASED IONIC LIQUIDS

BADANIA TRZECH CIECZY JONOWYCH NA BAZIE PIROLIDYNY METODĄ NISKOCZĘSTOTLIWOŚCIOWEJ SPEKTROSKOPII MECHANICZNEJ

In this work we present our recent results on three ionic liquids (ILs), which share bis(trifluoromethanesulfonyl)imide (TFSI) as anion and have different pyrrolidinium based cations. By means of a combination of mechanical spectroscopy and thermal analysis, many of the physical processes occurring during cooling down from the liquid phase, can be studied. Depending both on the diverse cation and the different thermal history, crystallization from the melt or glass transition, cold-crystallization, solid-solid phase transitions and thermally activated processes are observed. In one of the ILs, which could be easily undercooled, a prominent thermally activated peak could be observed above the glass transition. The temperature dependence of the relaxation time is approximated by a Vogel-Fulcher-Tamman equation, as usual for fragile glass forming liquids, and the apparent activation energy of $W = 0.36$ eV with a pre-exponential factor of the relaxation time $\tau_0 = 1.7 \cdot 10^{-13}$s were derived supposing jumps between asymmetrical potential wells. The kinetics of the crystallization processes have been studied in the framework of the Johnson-Mehl-Avrami-Kolmogorov theory and the Avrami parameters have been derived for both the crystallization from the melt and for the cold crystallization observed on heating.

Keywords: Ionic liquids, dynamic mechanical analysis, differential scanning calorimetry

W pracy przedstawiono najnowsze wyniki badań trzech cieczy jonowych (ILs), zbudowanych o anion bistriflimidowy (TFSI) i różne kationy pirolidyniowe. Za pomocą kombinacji spektroskopii mechanicznej i analizy termicznej można badać wiele procesów fizycznych występujących podczas schładzania z fazy ciekłej. W zależności od zróżnicowania kationów i różnic historii termicznej, można obserwować krystalizację cieczy lub zeszklenie, zimną krystalizację, przemiany fazowe w stanie stałym i procesy aktywowane termicznie. W jednej z ILs, którą można łatwo przechłodzić, obserwowano termicznie aktywowany pik powyżej temperatury zeszklenia. Zależność temperaturową czasu relaksacji aproksymowano równaniem Vogela-Fulchera-Tammana, co jest typowym podejściem stosowanym dla cieczy tworzących nietrwałe szkła, uzyskując pozorną energię aktywacji W = 0,36 eV i czas relaksacji $\tau_0 = 1.7 \cdot 10^{-13}$s przy założeniu przeskoków pomiędzy asymetrycznymi studniami potencjału. Kinetykę procesu krystalizacji badano w ramach teorii Johnson-Mehla-Avramiego-Kołmogorowa a parametry Avramiego zostały uzyskane zarówno dla krystalizacji z cieczy, jak i zimnej krystalizacji obserwowanej przy ogrzewaniu.

1. Introduction

Ionic liquids (ILs) are salts with melting points below 100°C. Due to their unique array of physico-chemical properties, such as negligible vapor pressure, high ionic conductivity, thermal and electrochemical stability and the ability to dissolve both organic and inorganic substances, they are being investigated for a wide range of applications, becoming key materials for environmentally friendly green chemistry [1,2]. ILs consist of large organic cations and inorganic smaller anions, which can be tuned for specific applications by making modest chemical changes to the functional groups on the ions. Information regarding the molecular dynamic behavior of each ion forming an IL is especially important because several of the basic properties of ILs are determined by their behaviors on a molecular level. The nature of the relaxation processes taking place in some ILs, in particular on those based on imidazolium cations, has been studied, mainly by means of nuclear magnetic resonance and broadband dielectric spectroscopy [3-5]. Since a low melting point is central in ILs, an understanding of the crystallization phenomena is extremely important. A study of the factors that influence the crystallization kinetics has been carried out in some archetypal ILs [6].

Among all applications, the use of ILs in electrochemical devices, such as Li-ion batteries, is one of the most challenging [7] and pyrrolidinium based ILs are one of the best choices as safe electrolytes for lithium cells [7]. The low-temperature phase transitions of some pyrrolidinium based ILs have been studied by means of differential scanning calorimetry (DSC) [8] and a glass transition around 190 K was reported for (1-butyl-1-methylpyrrolidinium bis(trifluoromethanesulfonyl)imide) (PYR_{14}-TFSI).

* PHYSICS DEPARTMENT, SAPIENZA UNIVERSITY OF ROME, P.LE A. MORO 5, 00185 ROMA, ITALY
** CNR-ISC, U.O.S. LA SAPIENZA, P.LE A. MORO 5, 00185 ROMA, ITALY
*** CHEMISTRY DEPARTMENT, SAPIENZA UNIVERSITY OF ROME, P.LE A. MORO 5, 00185 ROMA, ITALY

In this article we focus on three ionic liquids (ILs) which share bis(trifluoromethanesulfonyl)imide (TFSI) as anion and have different pyrrolidinium based cations, the only difference being the length of the side alkyl chain. The present work shows that is it possible, by means of a pocket which works as a substrate, to use low frequency mechanical spectroscopy to follow the main phase transitions occurring in ionic liquids by cooling down from room temperature, even in their liquid state. Moreover additional information with respect to the common calorimetric measurements is obtained. Indeed, previous works on mechanical properties of ionic liquids provide information either in their liquid or solid state.

2. Materials and experimental

Figure 1 shows the chemical structure of the three hydrophobic ILs investigated: PYR_{13}-TFSI (melting point at T_m = 285 K), PYR_{14}-TFSI (T_m = 267 K) and PYR_{15}-TFSI (T_m = 281 K). They were purchased from Solvionic (purity > 99.9%) and used as received.

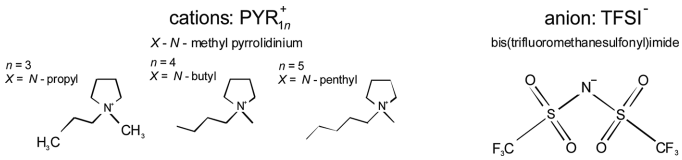

Fig. 1. Cations and anion chemical structures of the investigated ILs: PYR_{13}-TFSI, PYR_{14}-TFSI and PYR_{15}-TFSI

Dynamic mechanical analysis was carried out using a PerkinElmer DMA 8000 instrument. The samples, which are all in the liquid phase at room temperature, were spread into a stainless steel material pocket, supplied by PerkinElmer, with dimensions of 30 mm by 14 mm. The pocket, which is scored in the mid-point, was then folded in half and crimped closed to form a sandwich. Flexural vibration measurements were performed in three-point bending configuration. The storage modulus, M, and the elastic energy dissipation, tan δ, were measured in an inert argon atmosphere, at 1 Hz and 10 Hz, during cooling/heating at 4 K/min, between 150 and 330 K.

Differential scanning calorimetry (DSC) measurements were performed by a Mettler-Toledo DSC 821, under an inert nitrogen flux, cooling from room temperature down to 150 K, and then heating back to 300 K with a temperature rate of 4 K/min.

3. Results and discussion

Figures 2 and 3 show the DSC traces (upper part) and the DMA spectra (lower part) of the three samples, measured on cooling and heating respectively. The storage modulus is reported as relative variation with respect to the value at 300 K (M / $M_{300\ K}$ − 1), since it is not possible to separate the contribution of the IL from that of the pocket. However, the curves of both $M$and tan δ measured for the empty pocket are flat in the whole temperature range of the measurements (background curves in Fig. 2). Both DSC and DMA curves measured on cooling for PYR_{13}-TFSI and PYR_{15}-TFSI are consistent with the occurrence of samples crystallization around 230-240 K and 250 K respectively (exothermic peaks and stiffening jumps). The same samples melt, on heating, around 270-280 K (endothermic peaks and softening). Indeed, the melting processes for both samples occurs in at least two steps. The melting behavior of similar ILs has already been carefully investigated [9] and will not be discussed anymore here. The curves relative to PYR_{14}-TFSI are qualitatively different and reflect the well known dependence of the physicochemical properties of many ILs from the side alkyl chain length [10]. For our pyrrolidinium based ILs it appears that a chain of intermediate length minimizes the melting point and increases the tendency of the ionic liquid to form a glass rather than crystallize on cooling. This behavior has been observed also in other ILs and it is supposed to arise from the competition between long-range electrostatic forces and short-range chain-chain interaction [10]. On cooling, the DSC curve of PYR_{14}-TFSI shows only a small exothermic peak around 190 K, corresponding to the glass transition, as already reported in Ref. [8]. The anelastic spectrum shows, at the same temperature, a stiffening, with an increase of almost eight times of the storage modulus, and an intense peak of tan δ. On heating, the DSC trace shows an endothermic peak around 190 K, two exothermic peaks around 210 and 240 K and an intense endothermic peak around 265 K. In correspondence of all these peaks the DMA spectrum presents clear features on both the real and imaginary part of the elastic modulus. This phenomenology has been already interpreted straightforward in a previous paper [11], where we studied the temperature behavior of PYR_{14}-TFSI swelling a polyvinylidenfluoride membrane, providing information about the interaction of PYR_{14}-TFSI with the polymeric membrane. In particular, the abrupt stiffening observed on heating at T_{cc} ~210 K corresponds to the cold crystallization of the sample and below we will analyze the kinetic of this transformation. It is noticeably, that here the anelastic spectra are measured on the liquid and not on a composite system, thus avoiding any kind of interaction.

Now we shall briefly concentrate on the thermally activated peak observed in the anelastic spectrum of PYR_{14}-TFSI on cooling when the sample is in its supercooled liquid state. This process has a maximum around 230 K at 1 Hz and has never been reported by others. Figure 4 shows the anelastic spectra measured at two frequencies.On cooling, the DSC curve of PYR_{14}-TFSI shows only a small exothermic peak around 190 K, corresponding to the glass transition, as already reported in Ref. [8]. The anelastic spectrum shows, at the same temperature, a stiffening, with an increase of almost eight times of the storage modulus, and an intense peak of tan δ. On heating, the DSC trace shows an endothermic peak around 190 K, two exothermic peaks around 210 and 240 K and an intense endothermic peak around 265 K. In correspondence of all these peaks the DMA spectrum presents clear features on both the real and imaginary part of the elastic modulus. This phenomenology has been already interpreted straightforward in a previous paper [11], where we studied the temperature behavior of PYR_{14}-TFSI swelling a polyvinylidenfluoride membrane, providing information about the interaction of PYR_{14}-TFSI with the polymeric membrane. In particular, the abrupt stiffening observed on heating at T_{cc} ~210 K corresponds to the

cold crystallization of the sample and below we will analyze the kinetic of this transformation. It is noticeably, that here the anelastic spectra are measured on the liquid and not on a composite system, thus avoiding any kind of interaction.

Now we shall briefly concentrate on the thermally activated peak observed in the anelastic spectrum of PYR_{14}-TFSI on cooling when the sample is in its supercooled liquid state. This process has a maximum around 230 K at 1 Hz and has never been reported by others. Figure 4 shows the anelastic spectra measured at two frequencies.

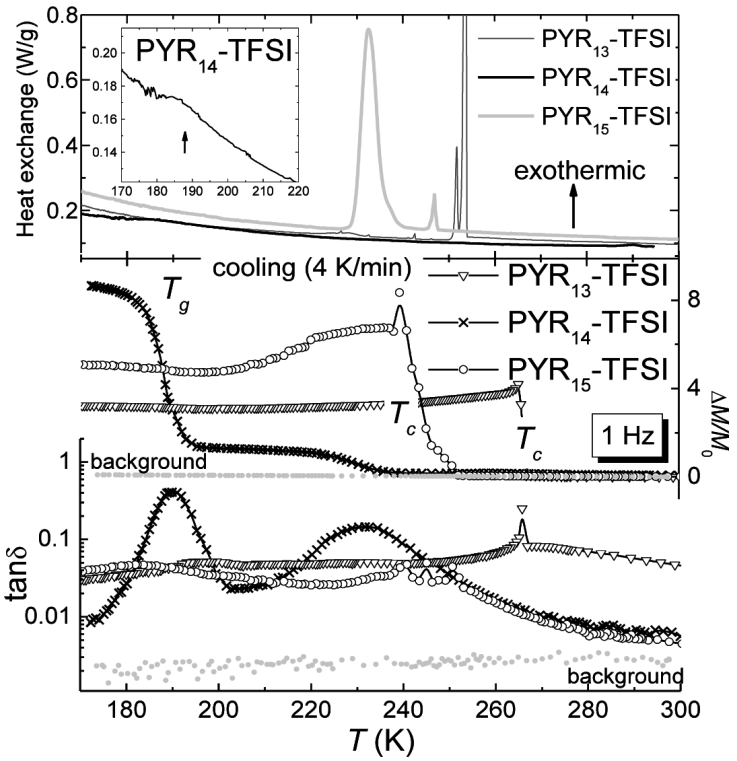

Fig. 2. DSC traces (upper part) and DMA spectra (lower part) of the three ILs, measured on cooling at 4 K/min

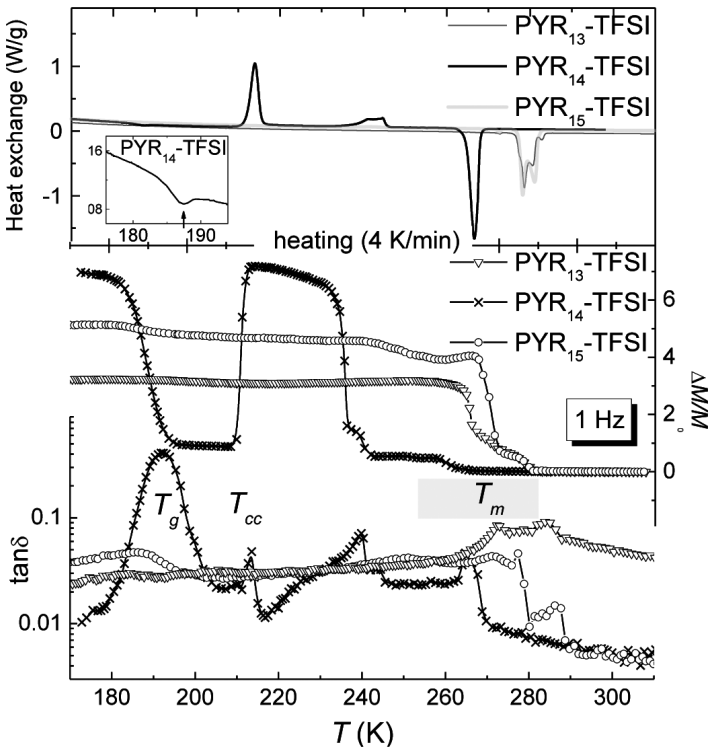

Fig. 3. DSC traces (upper part) and DMA spectra (lower part) of the three ILs, measured on heating at 4 K/min

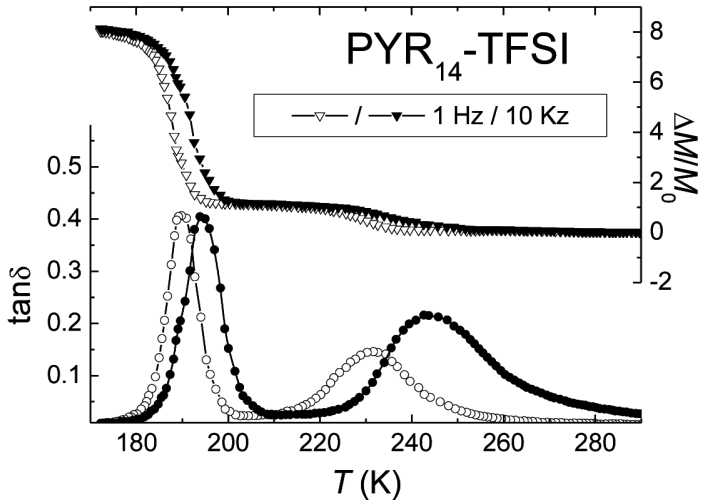

Fig. 4. DMA spectra of the pocket containing PYR_{14}-TFSI, measured at two frequencies

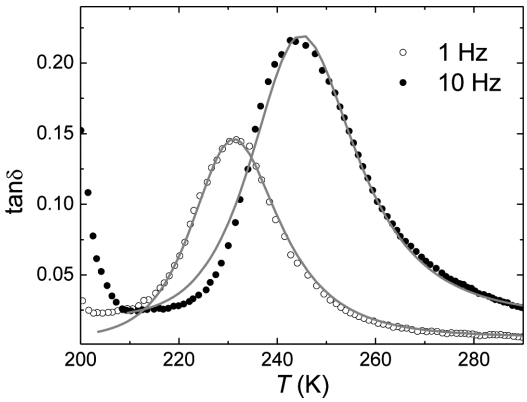

Fig. 5. Thermally activated peak in supercooled PYR_{14}-TFSI. The continuous line is a fit according to Eq. (1)

As showed in Fig. 5, we could achieve a reasonable fit to the data of the peak (continuous line) using the following expression, which is appropriated for jumps between asymmetrical potential wells:

$$\tan\delta = \frac{\Delta}{T\cosh\left(a/2k_BT\right)}\frac{1}{(\omega\tau)^{\alpha}+(\omega\tau)^{-\alpha}}, \qquad (1)$$

where τ is the relaxation time between two sites with the energy separation a, the constant Δ is proportional to the concentration of the relaxing species, to the elastic modulus and to the change in the local distortion, and α is the Fuoss–Kirkwood width parameter. In order to achieve a reasonable fit we had to impose to the relaxation time a Vogel-Fulcher-Tamman type dependence on temperature, that is, $\tau = \tau_0 \exp[W/k_B(T-T_0)]$, with $W = 0.36$ eV, $\tau_0 = 1.7\cdot 10^{-13}$s, $T_0 = 80$ K, $a = 26$ meV and $\alpha = 0.7$. The mechanism giving rise to this process is not clear, but several models have been suggested [12], considering either the existence of different conformers for the TFSI cation or the recognized presence in many ILs of nano-scale structural heterogeneities.

4. Crystallization and devetrification kinetics

In our previous study, on PYR_{14}-TFSI swelling a polyvinylidenfluoride membrane [11], we showed that the interaction with the membrane causes the crystallization of the ionic liquid either by cooling with a slow rate (0.5 K/min) or by prolonged isothermal treatments around 235 K. In that article we analyzed the crystallization kinetics of the composed system in terms of the Johnson-Mehl-Avrami-Kolmogorov (JMAK) equation [13] and determined the Avrami index and the activation energy for the crystallization. In what follows we extend the investigation to both the cold crystallization, observed on heating for pure PYR_{14}-TFSI, and the crystallization from the melt for pure PYR_{15}-TFSI. Figures 6 demonstrates the isothermal ($T = 200$ K) variation of the storage modulus during the cold crystallization of PYR_{14}-TFSI. The typical sigmoidal curve originates from the nucleation, which predominate at very short times and is followed by a period where growth dominates. At longer times the total growth rate decreases as a result of nuclei coalescing.

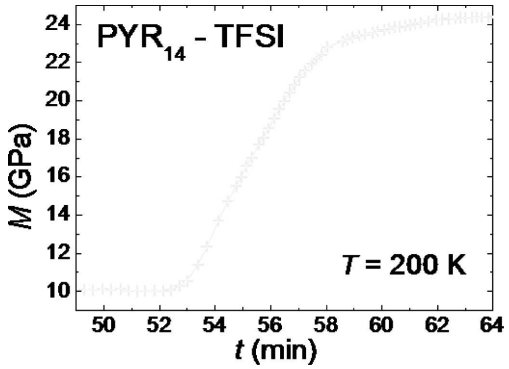

Fig. 6. Isothermal variation of the elastic modulus, measured with the DMA at 200 K, reached on heating, after cooling at 4 K/min down to 150 K

The basic assumption underlying the JMAK equation is that crystallization is a thermal or mass diffusion-controlled process, which involves nucleation and growth. In that frame-

work, for isothermal processes, the fraction χ of the sample transformed into the second phase is given by:

$$\chi = 1 - \exp(-kt^n), \tag{2}$$

where n is the constant Avrami exponent. If the nucleation is random, the rate constant k has an Arrhenius dependence on temperature, $k = k_0 \exp[E_a/RT]$, E_a and k_0 being the activation energy and the frequency factor of the crystallization process, respectively. The applicability of Eq. (2) can be verified by checking the linearity of a plot of $\ln[-\ln(1-\chi)]$ vs. $\ln(t)$. Supposing a diffusion controlled growth, the slope of the line, the Avrami exponent, should have the following values: $n = 1.5$, in the limit of zero nucleation rate; $n < 2.5$ for a decreasing nucleation rate; $n = 2.5$ in the case of constant nucleation rate; $n > 2.5$ for an increasing nucleation rate [6].

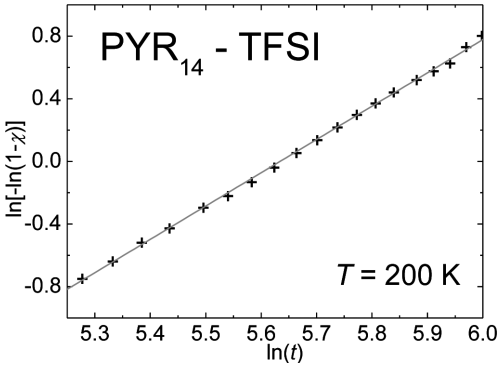

Fig. 7. Isothermal Avrami plot for the cold crystallization process, obtained from an isothermal DMA measurement at $T = 200$ K

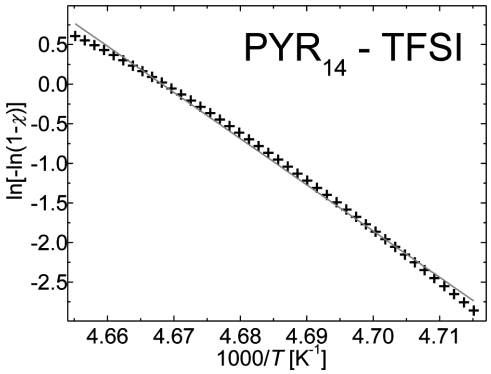

Fig. 8. Non-isothermal Avrami plot for the cold crystallization process. The continuous line shows the best linear fit curve

Figure 7 shows the plot of $\ln[-\ln(1-\chi)]$ vs. $\ln(t)$ obtained from an isothermal measurement carried out with the DMA at 200 K (reached on heating, after cooling the sample at 4 K/min down to 150 K). The fraction of sample transformed in the solid phase can be obtained as follows:

$$\chi(t) = \frac{M(t) - M_{\min}}{M_{\max} - M_{\min}}, \tag{3}$$

where $M_{\min}$ and $M_{\max}$ are the values of the elastic modulus before the beginning and after the end of the crystallization. In Fig. 7 the applicability of Eq. (2) is proven, as explained above, and the Avrami index $n = 2.13 \pm 0.02$ is obtained. The fraction of sample transformed can be obtained also from an isothermal DSC measurement by the ratio between of heat exchanged at a given time, $S(t)$, and the total heat exchanged in the cold crystallization process, i.e. $\chi(t) = S(t)/S_0$, where the integrals $S(t)$ and S_0 are calculated between the onset time and time t and between the onset and the ending time of the peak, respectively. By the same plot of Fig. 7 (not reported here) we obtained $n = 2.12 \pm 0.01$, which coincides, within the experimental errors, with the value obtained from the DMA measurements and therefore increases the confidence in this analysis.

Taking into account the form of $k(T)$, differentiating Eq. (2) with respect to time and then integrating with non-isothermal conditions, leads to [6]:

$$\ln[-\ln(1-\chi)] = -\frac{nE_a}{RT} - C(T), \tag{4}$$

where $C(T)$ is a term which contains the temperature rate and an approximation of the temperature integral of the Arrhenius factor, which cannot be integrated analytically. For some archetypal ILs it has been shown [6] that is reasonable to assume $C(T) \approx$ constant, as proved from the fairly linearity of a plot like that reported in Fig. 8. With this hypothesis, the slope of the line gives nE_a/R and then, taking into account the value of n calculated before, one obtains the activation energy.

The same analysis has been also carried out for the crystallization from the melt observed in PYR_{15}-TFSI around 250 K. Both isothermal ($T = 255$ K) and non-isothermal DSC and DMA data have been elaborated as above and the estimated Avrami parameters are reported in Table 1.

TABLE 1

Avrami parameters for the crystallization from the melt of PYR_{15}-TFSI and from the cold crystallization of PYR_{14}-TFSI

Sample	n	E_a
PYR_{14}-TFSI	2.13 ± 0.02	231 ± 4 kJ·mol^{-1}
PYR_{15}-TFSI	1.85 ± 0.05	161 ± 5 kJ·mol^{-1}

To conclude, providing that the assumption of diffusion controlled growth is correct and JMAK theory is applicable, the values of the Avrami index suggest that for both the ionic liquids studied growth occurs with a decreasing nucleation rate. This is probably due to the heat released at the interface, which causes a temperature rise in the surrounding liquid and therefore a decrease in the nucleation rate in those regions of the liquid.

5. Summary

We reported the results of a study, carried out by means of DMA and DSC, of the phase transitions of three pure ionic liquids, which share TFSI as anion and have pyrrolidinium based cations, differing only for the length of the side alkyl chain. We found that PYR_{14}-TFSI, with the intermediate chain length, can be easily undercooled down to the glass transition observed around 190 K. A prominent thermally activated peak can be observed around 230 K at 1 Hz, when the sample is in the supercooled liquid state. An acceptable fit has been obtained by supposing that the relaxing entity jumps between asymmetric wells, separated by an activation

energy of the order of 0.36 eV and with a relaxation time which follows a Vogel-Fulcher-Tamman law ($\tau_0 = 1.7 \cdot 10^{-13}$s, $T_0 = 80$ K). The sample of PYR_{14}-TFSI crystallizes around 200 K on heating from the glassy state. An analysis of the crystallization kinetics for both the cold-crystallization process of PYR_{14}-TFSI and the crystallization from the melt of PYR_{15}-TFSI, has been carried out on the basis of the Johnson-Mehl-Avrami-Kolmogorov equation. The values of the activation energy and the Avrami index have been derived and the latter suggest that for both the ionic liquids studied growth occurs with a decreasing nucleation rate.

REFERENCES

[1] B. Kirchner (ed.), Ionic Liquids. Topics in Current Chemistry **290**, Springer, Berlin, 2009.

[2] M. Armand, F. Endres, D.R. MacFarlane, H. Ohno, B. Scrosati, Ionic-liquid materials for the electrochemical challenges of the future, Nat. Mater. **8**, 621-629 (2009).

[3] A. Rivera, A. Brodin, A. Pugachev, E.A. Rössler, Orientational and translational dynamics in room temperature ionic liquids, J. Chem. Phys. **126**, 114503-1-7 (2007).

[4] C. Krause, J.R. Sangoro, C. Iacob, F. Kremer, Charge transport and dipolar relaxations in imidazolium-based ionic liquids, J. Phys. Chem. B **113**, 10641-10649 (2009).

[5] K. Nakamura, T. Shikata, Systematic dielectric and NMR study of the ionic liquid 1-Alkyl-3-Methyl imidazolium, Chem. Phys. Chem. **11**, 285-294 (2010).

[6] J. Pas, M.S. Dargusch, D.R. MacFarlane, Crystallization kinetics of some archetypal ionic liquids: isothermal and non-isothermal determination of the Avrami exponent, Phys. Chem. Chem. Phys. **13**, 12033-12040 (2011).

[7] M.A. Navarra, Ionic liquids as safe electrolyte components for Li-metal and Li-ion batteries, MRS Bull. **38**, 548-553 (2013).

[8] A. Martinelli, A. Matic, P. Jacobsson, L. Borjesson, Phase behavior and ionic conductivity in Lithium bi-(trifluoromethanesulfonyl)imide-doped ionic liquids of the pyrrolidinium cation and bis(trifluoromethanesulfonyl)imide anion, J. Phys. Chem. B **113**, 11247-11251 (2009).

[9] M. Kunze, M. Montanino, G.B. Appetecchi, S. Jeong, M. Schönhoff, M. Winter, S. Passerini, Melting behavior and ionic conductivity in hydrophobic ionic liquids, J. Phys. Chem. A **114**, 1776-1782 (2010).

[10] H. Tokuda, K. Hayamizu, K. Ishii, M. Susan, M. Watanabe, Physicochemical properties and structures of room temperature ionic liquids. 2, Variation of alkyl chain length in imidazolium cation, J. Phys. Chem. C **109**, 6103-6110 (2005).

[11] F.M. Vitucci, D. Manzo, M.A. Navarra, O. Palumbo, F. Trequattrini, S. Panero, P. Bruni, F. Croce, A. Paolone, Low-temperature phase transitions of 1-butyl-1-methylpyrrolidinium bis(trifluoromethanesulfonyl)imide swelling a polyvinylidenefluoride electrospun membrane, J. Phys. Chem. C **118**, 5749-5755 (2014).

[12] F. Trequattrini, A. Paolone, O. Palumbo, F.M. Vitucci, Relaxation dynamics and phase transitions in PYR_{14}-TFSI, J. Phys. Chem. A, to be published.

[13] K.F. Kelton, A.L. Greer, Nucleation in condensed matter, Elsevier, Amsterdam, 2010.

Received: 20 October 2014.